

Aqueous Solutions for Low-Temperature Photoannealing of Functional Oxide Films: Reaching the 400 °C Si-Technology Integration Barrier

Christopher De Dobbelaere,[†] Maria Lourdes Calzada,[‡] Ricardo Jiménez,[‡] Jesús Ricote,[‡] Iñigo Bretos,[‡] Jules Mullens,[†] An Hardy,[†] and Marlies K. Van Bael^{*,†}

[†]Inorganic and Physical Chemistry Group, Institute for Materials Research, Universiteit Hasselt, IMEC vzw, Division IMOMECE, B-3590 Diepenbeek, Belgium

[‡]Instituto de Ciencia de Materiales de Madrid, C.S.I.C., Cantoblanco, E-28049 Madrid, Spain

 Supporting Information

ABSTRACT: Functional oxide films were obtained at low temperature by combination of aqueous precursors and a UV-assisted annealing process (aqueous photochemical solution deposition). For a PbTiO₃ model system, functional ferroelectric perovskite films were prepared at only 400 °C, a temperature compatible with the current Si-technology demands. Intrinsically photosensitive and environmentally friendly aqueous precursors can be prepared for most of the functional multimetal oxides, as additionally demonstrated here for multiferroic BiFeO₃, yielding virtually unlimited possibilities for this low-temperature fabrication technology.

Metal oxide films are indispensable in modern nanoelectronic, memory, biosensing, energy storage, and photovoltaic applications. To manufacture such a large variety of functional films, chemical solution deposition (CSD) routes, which require postdeposition annealing at high temperatures (>600 °C), are often the method of choice because of easy composition control, low cost, and large-area deposition.¹ However, in view of today's environmental and economic solicitude, as well as to ensure technical compatibility with thermally unstable Si-based semiconductor substrates and stacks, thermal budgets should be kept as low as possible. Low-temperature processing is a critical issue that constitutes a technological milestone for the realistic integration of any functional metal oxide into electronic devices.

Metal alkoxide-based CSD routes use organic solvents such as 2-methoxyethanol, which is a possible human teratogen, contributes to photochemical smog, and is listed in the U.S. Clean Air Act as a substance to be avoided. Although less hazardous media have been reported,^{2–5} the issue of solvent toxicity has been largely overcome by the recent development of aqueous CSD. Previous work has demonstrated that many (multi)metal oxide systems can be synthesized from these innocuous water-based precursor systems.^{6–9} Insensitivity of the metal ions toward hydrolysis and condensation is ensured by the formation of water-soluble α -hydroxycarboxylato metal complexes using chelating carboxylic acids such as citric acid. Although aqueous CSD is a potent replacement for traditional sol–gel systems from the toxicity point of view, high annealing temperatures

typical for any CSD route are still required for aqueous-precursor-derived films.

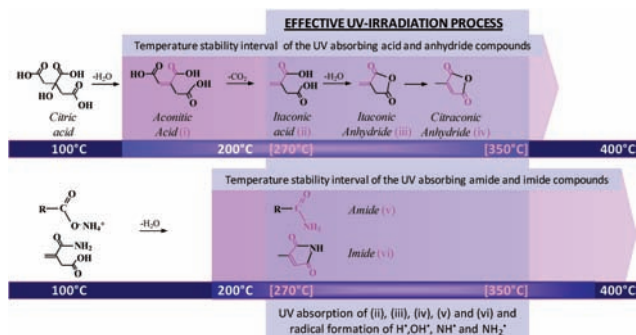
The use of UV irradiation during the thermal decomposition of solution-deposited films in a photochemical solution deposition (PCSD) process has been demonstrated to be a valuable technique for reducing annealing temperatures of sol–gel-processed ferroelectric oxide films while preserving their functional properties.^{10–14} However, until now it has only been applied to conventional alkoxide-based precursors containing external UV absorber species.^{10,15} The present study demonstrates that the undesired and superfluous addition of photosensitive compounds is not needed for water-based precursor systems. Aqueous carboxylato precursors have an enhanced and intrinsic UV sensitivity in a wide temperature window, resulting in a significant reduction of the thermal requirements when they are subjected to a PCSD process. Low-temperature processing avoids the emission of toxic volatiles from the precursors¹⁴ and makes the integration of functional multimetal oxide systems in complementary metal oxide semiconductors (CMOS) feasible.

The potential of aqueous citrato(-peroxo) precursors in UV-assisted photoannealing processes is demonstrated herein for the first time using lead titanate (PbTiO₃) as a model system.¹⁶ Although some lead-free compounds appear to be promising,¹⁷ lead-based perovskites still dominate the market of ferro-piezoelectric components.¹⁸ To date, few publications have demonstrated adequate functionality for (multi)metal oxide thin films using a maximum temperature below 450 °C.^{11,14,19,20}

The thermal decomposition of aqueous ammonium metal citrate precursors has been studied previously.^{21–23} In a first temperature region ($T < 270$ °C), the uncoordinated ammonium citrate matrix surrounding the metal ion complexes decomposes, while the direct coordination of metal ions does not change. Several endothermic processes occur, including decomposition of noncoordinated ammonium carboxylate groups into carboxylic acids and NH₃, amide formation, dehydroxylation of α -hydroxycarboxylates followed by anhydride formation, and decarboxylation of the remaining unsaturated carboxylic acids and their evaporation,²¹ all of which result in the formation of UV-absorbing carboxylate derivatives, (cyclic) anhydrides, amides, and imides [Figure S1 in the Supporting Information (SI)]. However, UV

Received: April 18, 2011

Published: August 01, 2011

Scheme 1. Thermal Decomposition of an Aqueous Precursor Gel^a

^a See refs 21–23. The UV-absorbing species formed in the decomposition are indicated. Species (ii)–(vi) are stable between 270 and 350 °C, where the maximum absorption and effectiveness of UV irradiation for the fabrication of oxide films at low temperature is demonstrated. Reactive radicals appear in this interval as byproducts of the photoinduced reactions. To generalize the decomposition process, pure citric acid is presented; in the aqueous system, citric acid is coordinated to the metal ions or ammonium cations. Brackets indicate UV irradiation.

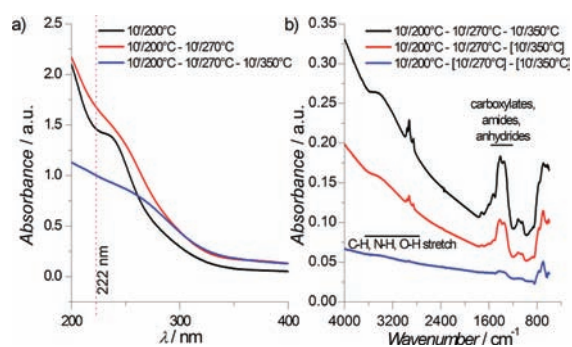


Figure 1. (a) UV–vis absorption spectra of PbTiO₃ precursor films after each step of the optimized thermal profile. UV absorption is ensured in the wavelength region of the UV source (222 nm). (b) GATR-FTIR spectra of PbTiO₃ precursor films on platinum-coated silicon substrates after various thermal and UV treatments. Almost all of the organic compounds are eliminated for films treated using the optimal thermal profile. Brackets indicate UV irradiation.

irradiation in this temperature region results in film blistering due to the excessive decomposition of UV-absorbing compounds (Figure S2). At higher temperatures (270 °C < *T* < 420 °C), breakdown of the α -hydroxy coordination of the metal ion occurs, producing carboxylate derivatives comparable to those formed during the decomposition of pure citric acid and ammonium citrate (Scheme 1).

Grazing-angle attenuated total reflection Fourier transform IR (GATR-FTIR) spectroscopy confirms that UV irradiation results in a decrease in the organic content of the film (Figure 1b). Moreover, UV absorption spectra of lead titanate precursor films treated at 270 and 350 °C show that absorption at \sim 222 nm is ensured at all stages before the final temperature treatment (Figure 1a). Closer to and above 400 °C, both the metal ion carboxylates and the residual organic matrix in the gel further decompose, and metal oxide bonds are formed.

During the UV-assisted thermal decomposition in oxygen, UV photons form ozone (O₃) and active oxygen [O(¹D)]. O₃ advances the oxidation of organic compounds present (i.e.,

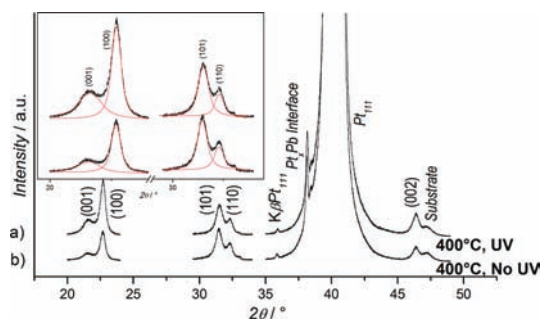


Figure 2. XRD peaks of single-phase tetragonal PbTiO₃ (JCPDS no. 06-0452) on platinum-coated silicon substrates: (a) UV-irradiated film treated at 400 °C; (b) non-UV-irradiated film treated at 400 °C.

ozonolysis), whereas active oxygen improves the stoichiometry of the crystalline phase and decreases the amounts of defects, vacancies, and leakage currents in the film.^{24,25} As a result of the photosensitivity of the precursor system, the excitation of photoactive groups formed during decomposition also induces the dissociation of chemical bonds and the low-temperature formation of metal–O–metal bonds.²⁶ Because of the precursors' intrinsic UV absorption originating from (partially decomposed) citrato(-peroxo) metal ion complexes (Scheme 1 and Figure 1a), the addition of any external photoinitiator becomes superfluous. As a result of dehydroxylation and combustion reactions occurring during precursor decomposition,^{21,23,27} water is released in a wide temperature window. Photolysis of water leads to the formation of highly reactive atomic hydrogen and hydroxyl radicals.^{28,29} Also, photolysis of ammonia released during the decomposition of ammonium carboxylates or amides²¹ leads to the formation of reactive H, NH, and NH₂ radicals.^{29,30} In contrast to other precursor systems,^{10,11,14,15} films derived from aqueous precursor systems are thus UV-active in a wide temperature window.

Following an optimized thermal profile, all of the films (deposited on Pt/IrO₂/Ir/SiO₂/Si) are UV-irradiated at 270 and 350 °C and annealed at 400 °C (Scheme 1; also see page S7 in the SI). To benefit from the enhanced decomposition of organics and the formation of O(¹D) radicals, treatments are carried out in oxygen. X-ray diffraction (XRD) indicates single-phase PbTiO₃, with no different orientation or phase purity for films treated with or without UV irradiation (Figure 2 and Figure S3). The crystallite sizes and microstrains derived from XRD data are identical, and narrow grain size distributions are obtained according to atomic force microscopy (AFM) topography analysis of the films (Table 1; AFM images are shown in Figure S4).

However, the relative intensities of the perovskite diffraction peaks are clearly higher for the UV-treated film, indicating a larger amount of crystalline phase (Figure 2 inset and Table 1). In addition, the irradiated film is thinner than its nonirradiated counterpart, suggesting a larger degree of crystallization/sintering. The greater thickness of the nonirradiated film may indicate a lower bulk density due to a larger porosity or greater amounts of amorphous or poorly crystallized phases of lower density arising from the low-atomic-weight carbonaceous compounds that are still not decomposed (Figure S5).

A film with a higher percentage of fully crystallized phase and degree of sintering is associated with improved functional properties. For all films annealed at 400 °C, ferroelectric behavior is confirmed by the shape of the experimental hysteresis loop (black curves in Figure 3a–c), from which the ferroelectric

Table 1. Film Thickness, Grain Size Measured with AFM, and Crystalline Characteristics Obtained from XRD Patterns of PbTiO₃ Films on Platinum-Coated Silicon Substrates Prepared at 400 °C with and without UV Irradiation

	film thickness ^a	AFM lateral grain size ^a	XRD characteristics		
			crystallite size ^a	microstrain	intensities ^b
UV	155	60–80	11 ± 1	−37 × 10 ^{−4}	$I_{001} \approx 37.1$ $I_{100} \approx 137.7$
no UV	250	60–80	11 ± 1	−37 × 10 ^{−4}	$I_{001} \approx 16.2$ $I_{100} \approx 72.2$

^a In nm. ^b Intensities (counts) of the (001) and (100) peaks.

switching contribution can be extracted (red lines).³¹ The film obtained from a 16 mol % excess lead precursor solution that was UV-irradiated and crystallized in oxygen has the most advantageous ferroelectric properties: $P_r = 8.8 \mu\text{C cm}^{-2}$, $P_s = 10.4 \mu\text{C cm}^{-2}$, and $E_c = 320 \text{ kV cm}^{-1}$ (Figure 3a). The corresponding film without photoactivation shows a much weaker response: $P_r = 1.3 \mu\text{C cm}^{-2}$, $P_s = 1.7 \mu\text{C cm}^{-2}$, and $E_c = 278 \text{ kV cm}^{-1}$ (Figure 3b). In the absence of UV light, no reactive species are formed, no photolysis of water or ammonia occurs, and no carboxylates (derivatives) are photoactivated. Overall, more organics or amorphous phases remain present at the same temperature, resulting in smaller amounts of perovskite phases and a larger number of defects.

The addition of excess lead to a stoichiometric PbTiO₃ precursor usually helps reduce the crystallization temperature of the film and increase the amount of perovskite phase, improving its ferroelectric properties.¹⁴ However, even UV-treated films prepared from a nominally stoichiometric precursor solution at 400 °C show a ferroelectric response: $P_r = 3.0 \mu\text{C cm}^{-2}$, $P_s = 5.2 \mu\text{C cm}^{-2}$, and $E_c = 165 \text{ kV cm}^{-1}$ (Figure 3c). These values are better than those obtained from the 16 mol % solution without UV irradiation, indicating the superior effect of UV irradiation.

Films with excess lead and UV irradiation crystallized at temperatures below 400 °C (375 °C) are not ferroelectric at all (Figure 3d), despite the fact that XRD indicates the presence of a (less) crystalline perovskite phase (Figure S3d).

AFM and XRD analyses indicate that films prepared at 400 °C (16 mol % excess lead) have grains of similar size irrespective of the use of UV irradiation but more crystalline phase when UV is applied (Table 1 and Figure 2). This can also be inferred from the cross-sectional scanning electron microscopy (SEM) images in Figure S5 and is reflected in the different thicknesses of the two films (Table 1). The lower crystallinity in the nonirradiated film is associated with a higher porosity and the presence of organics/amorphous phases still remaining in the bulk film. Nonferroelectric phases and organic compounds damage the ferroelectric response of the film, but in addition, the low degree of sintering and low density imply poor contact among the ferroelectric grains. This impedes the growth of ferroelectric switching domains throughout the grain boundaries and results in a lower polarization value. Although the ferroelectric responses for the UV-irradiated films are inferior to those obtained after conventional crystallization (>600 °C), they do fulfill the requirements needed for a realistic integration of this multifunctional oxide film at temperatures compatible with current silicon technology trends.¹⁸

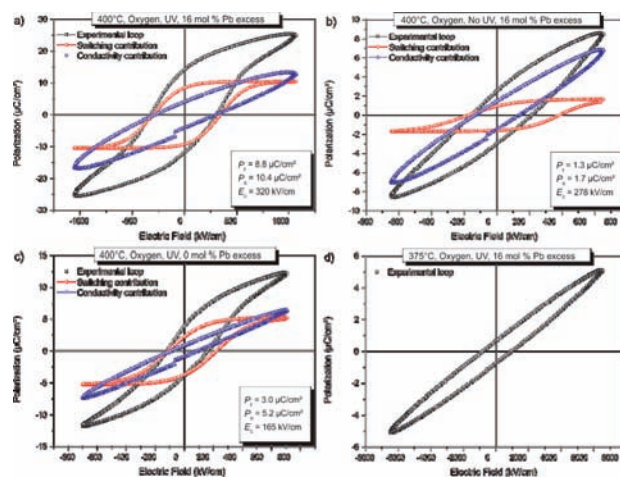


Figure 3. Ferroelectric responses for different PbTiO₃ films on platinum: black □, experimental loop; red ○, ferroelectric switching contribution; blue △, nonferroelectric conductivity contribution.

To illustrate the general applicability of the aqueous PCSD method to the low-temperature fabrication of oxide films, multi-ferroic bismuth ferrite (BiFeO₃) was investigated. UV–vis absorption spectra of solution-deposited BiFeO₃ precursor layers show that UV-absorbing films are obtained during all stages of the thermal profile of Scheme 1 (Figure 4a). UV absorbance is connected to $\pi \rightarrow \pi^*$ transitions inside the aqueous citrate complex (and its decomposition products) and thus is intrinsically linked to the chemical nature of the ligand coordinated to the metal ion. The general behavior of these aqueous systems is thus independent of the oxide composition. As for the PbTiO₃ precursor, GATR-FTIR spectra of BiFeO₃ precursor films on platinum-coated silicon substrates indicate the effectiveness of UV irradiation on the early decomposition of organics (Figure 4b). Moreover, the metal oxide film is crystallized at a lower temperature, as shown by the XRD patterns of the BiFeO₃ film prepared at 400 °C with and without UV irradiation (Figure 4c).

To summarize, functional thin films can be fabricated at a low temperature compatible with the current Si-technology demands using α -hydroxycarboxylato-based aqueous precursors in a photochemical solution deposition (aqueous PCSD) process. In these systems, the formation of chemical species with strong UV absorption is ensured by the chemical nature of the precursor. Intrinsically photosensitive products are formed during thermal decomposition of the films, making external photoinitiators superfluous. An appropriate design of the thermal profile used for the crystallization of the films results in efficient UV irradiation in a thermal window between 270 and 350 °C. In this region, water, ammonia, (cyclic) anhydrides, amides, and imides are formed that enhance the absorption of UV light and the amorphous-to-crystalline conversion of the film. In addition, ozonolysis resulting from UV irradiation in an oxygen atmosphere enhances precursor decomposition and crystallization of a less-defective perovskite phase. Therefore, PbTiO₃ perovskite films with ferroelectric properties appropriate for their integration into functional microelectronic devices can be fabricated at only 400 °C. Since this final temperature is below standard CMOS requirements (<450 °C), processing issues such as dopant diffusion in Si, NiSi junction contact destruction, and the emission of toxic compounds are avoided. Furthermore, the reported preparation method employs purely water-based

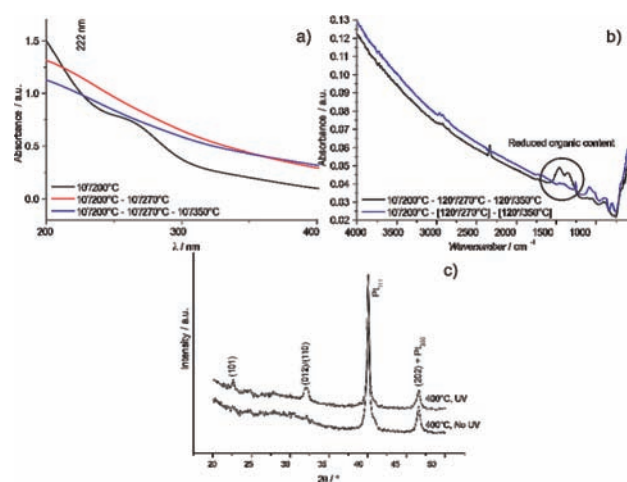


Figure 4. (a) UV–vis absorption spectra of BiFeO₃ precursor films after each step of the thermal profile. (b) GATR-FTIR spectra of BiFeO₃ precursor films on platinum-coated silicon with different thermal and UV treatments. Brackets indicate UV irradiation. (c) XRD patterns of BiFeO₃ (JCPDS no. 86-1518) films annealed at 400 °C (oxygen, 1 h) with and without UV treatment.

systems that make the overall process economically and ecologically appealing. The intrinsic photosensitivity of α -hydroxycarboxylato metal complexes and their decomposition products make this synthesis route generally applicable to any metal oxide compound, as shown for the multiferroic BiFeO₃ precursor system. Therefore, we envisage a wealth of applications for the aqueous PCSD method in the fabrication and integration of all kinds of (multi)metal oxides into microelectronics.

■ ASSOCIATED CONTENT

S Supporting Information. Experimental details; UV–vis spectra; AFM topographies; GIXRD patterns; and SEM images of UV- and non-UV-treated films. This material is available free of charge via the Internet at <http://pubs.acs.org>.

■ AUTHOR INFORMATION

Corresponding Author
marlies.vanbael@uhasselt.be

■ ACKNOWLEDGMENT

A.H. is a postdoctoral research fellow of the Research Foundation-Flanders (FWO Vlaanderen). I.B. is a postdoctoral research fellow financed by the JAE-Doc CSIC Spanish Program. The Spanish authors are grateful for the partial financial support from the Spanish Projects MAT2010-15365.

■ REFERENCES

- (1) Schwartz, R. W.; Schneller, T.; Waser, R. C. *R. Chim.* **2004**, *7*, 433.
- (2) Wang, J. Z.; Hu, Y.; Liu, J.; Wang, J. Z.; Chen, Z. Y. *J. Am. Ceram. Soc.* **2005**, *88*, 34.
- (3) Phillips, N. J.; Calzada, M. L.; Milne, S. J. *J. Non-Cryst. Solids* **1992**, *147*, 285.
- (4) Zhen, M.; Jihong, Y.; Sheng, D. *Adv. Mater.* **2010**, *22*, 261.

(5) Anastas, P. T.; Warner, J. C. *Green Chemistry: Theory and Practice*; Oxford University Press: New York, 1998.

(6) Van Werde, K.; Vanhoyland, G.; Nelis, D.; Mondelaers, D.; Van Bael, M. K.; Mullens, J.; Van Poucke, L. C. *J. Mater. Chem.* **2001**, *11*, 1192.

(7) *Handbook of Nanoceramics and Their Based Nanodevices*, 1st ed.; Tseng, T.-Y., Nalwa, H. S., Eds.; American Scientific Publishers: Valencia, CA, 2006; Vol. 1.

(8) Hardy, A.; D'Haen, J.; Goux, L.; Wouters, D. J.; Van Bael, M.; Van den Rul, H.; Mullens, J. *Chem. Mater.* **2007**, *19*, 2994.

(9) De Dobbelaere, C.; Hardy, A.; D'Haen, J.; Van den Rul, H.; Van Bael, M. K.; Mullens, J. *J. Eur. Ceram. Soc.* **2009**, *29*, 1703.

(10) Calzada, M. L.; Gonzalez, A.; Poyato, R.; Pardo, L. *J. Mater. Chem.* **2003**, *13*, 1451.

(11) Calzada, M. L.; Bretos, I.; Jimenez, R.; Guillon, H.; Pardo, L. *Adv. Mater.* **2004**, *16*, 1620.

(12) Shannigrahi, S. R.; Lim, X.; Tay, F. E. H. *J. Appl. Phys.* **2007**, *101*, No. 024107.

(13) Dunn, S.; Jones, P. M.; Gallardo, D. E. *J. Am. Chem. Soc.* **2007**, *129*, 8724.

(14) Bretos, I.; Jimenez, R.; Garcia-Lopez, J.; Pardo, L.; Calzada, M. L. *Chem. Mater.* **2008**, *20*, 5731.

(15) Uozumi, G.; Kageyama, K.; Atsuki, T.; Soyama, N.; Uchida, H.; Ogi, K. *Jpn. J. Appl. Phys., Part 1* **1999**, *38*, 5350.

(16) Scott, J. F. *Science* **2007**, *315*, 954.

(17) Saito, Y.; Takao, H.; Tani, T.; Nonoyama, T.; Takatori, K.; Homma, T.; Nagaya, T.; Nakamura, M. *Nature* **2004**, *432*, 84.

(18) Semiconductor Industry Association. International Roadmap for Semiconductors (ITRS). <http://www.itrs.net/links/2009ITRS/Home2009.htm> (accessed April 18, 2011).

(19) Wu, A.; Vilarinho, P. M.; Reaney, I.; Salvado, I. M. M. *Chem. Mater.* **2003**, *15*, 1147.

(20) Koscec, M.; Malic, B.; Mandeljc, M. *Mater. Sci. Semicond. Process.* **2002**, *5*, 97.

(21) Van Werde, K.; Vanhoyland, G.; Mondelaers, D.; Van den Rul, H.; Van Bael, M. K.; Mullens, J.; Van Poucke, L. C. *J. Mater. Sci.* **2007**, *42*, 624.

(22) Van Werde, K.; Mondelaers, D.; Vanhoyland, G.; Nelis, D.; Van Bael, M. K.; Mullens, J.; Van Poucke, L. C.; Van der Veken, B.; Desseyne, H. O. *J. Mater. Sci.* **2002**, *37*, 81.

(23) Hardy, A.; Van Werde, K.; Vanhoyland, G.; Van Bael, M. K.; Mullens, J.; Van Poucke, L. C. *Thermochim. Acta* **2003**, *397*, 143.

(24) Boyd, I. W.; Zhang, J. Y. *Solid-State Electron.* **2001**, *45*, 1413.

(25) Zhang, Y.; Terrill, R. H.; Bohn, P. W. *Chem. Mater.* **1999**, *11*, 2191.

(26) *Handbook of Sol–Gel Science and Technology*; Sakka, S., Ed.; Kluwer: Dordrecht, The Netherlands, 2005; Vol. 1.

(27) Truijen, I.; Hardy, A.; Van Bael, M. K.; Van den Rul, H.; Mullens, J. *Thermochim. Acta* **2007**, *456*, 38.

(28) Van de Leest, R. E. *Appl. Surf. Sci.* **1995**, *86*, 278.

(29) McNesby, J. R.; Okabe, H.; Tanaka, I. *J. Chem. Phys.* **1962**, *36*, 605.

(30) Kenner, R. D.; Rohrer, F.; Stuhl, F. *J. Chem. Phys.* **1987**, *86*, 2036.

(31) Jimenez, R.; Alemany, C.; Calzada, M. L.; Gonzalez, A.; Ricote, J.; Mendiola, J. *Appl. Phys. A: Mater. Sci. Process.* **2002**, *75*, 607.